Filtering and Left Ventricle Segmentation of the Fetal Heart in Ultrasound Images

Lorena Vargas-Quintero[a], Boris Escalante-Ramírez[a]
[a] Advanced Laboratory of Image Processing – Signal Processing Dep.–Engineering Faculty
Universidad Nacional Autónoma de México, México D.F.

ABSTRACT

In this paper, we propose to use filtering methods and a segmentation algorithm to analyze the fetal heart in ultrasound images. Since speckle noise makes difficult the analysis of ultrasound images, the filtering process becomes a useful task in this application. The filtering techniques considered in this work assume that the speckle noise is a random variable with a Rayleigh distribution. We use two multiresolution methods: one based on wavelet decomposition and the other based on the Hermite transform. The filtering process is used as a way to strengthen the performance of the segmentation task. For the wavelet-based approach, a Bayesian estimator at subband level for pixel classification is employed. The Hermite method computes a mask to find those pixels that are corrupted by speckle. We picked out a method based on a deformable model or "snake" to evaluate the influence of the filtering techniques in the segmentation task. We selected the left ventricle in fetal echocardiographic images as structure of analysis. Quantitative evaluation is addressed to assess the performance of the filtering process and the segmentation task.

Keywords: Speckle, Hermite Transform, Wavelet Transform, Ultrasound image, Active Contour.

1. INTRODUCTION

Cardiac diseases have been one of the main causes of death in the last years[1, 2]. The early detection of affections in the heart still constitutes a great challenge for physicians, particularly when the studies are addressed to fetuses. Medical images have become indispensable tools to carry out efficient evaluations of the cardiac function. The principal medical image modality applied to fetal analysis is ultrasound because of no-ionizing radiation is needed. Although ultrasound images are extensively employed for all the applications of medical analysis due to their low cost and safety procedure, they still present many disadvantages for clinical interpretation. The reasons are the low contrast and speckle patterns[3].

Chamber segmentations represent some of the principal tasks to assess the functions of the heart [4, 5]. Even though the segmentation of cardiac structures has been treated for many years[6-8], it is still an open issue. The main reason is the great variability that we can find in the heart. For ultrasound systems, complexity level for the segmentation task increases due to the above reasons. Considering that our goal is to analyze fetal echocardiographic images, the segmentation becomes even more complicated. In medical applications, deformable models have reached special attention to address the segmentation task[9-12]. One of the most accepted deformable models is the active contour proposed by Kass et al.[9] which is known as "snake". In the case of cardiac fetal analysis, several approaches have been also used to segment different structures[8]. Despite many researchers have demonstrated that deformable models have several limitations[9-12], we opted to use "snakes" for the chamber segmentation in fetal echocardiographic images. The reason is that we wish to evaluate the effect of a filtering process in the segmentation task.

Generally speaking, filtering processes on ultrasound images are commonly applied before a segmentation process in order to reach better results [13-22]. Several methods have been proposed to filter and enhance ultrasound images[13-22] in the last twenty years. Most of them are based on multiresolution decomposition[15-17, 20] and statistical interpretation[14, 18]. In our work, we used two multiscale-based approaches to filter our images. The first one is the wavelet-based method proposed by Gupta et al. [21] and the second one is a Hermite-based method which was exposed in [23-24].

IX International Seminar on Medical Information Processing and Analysis, edited by
Jorge Brieva, Boris Escalante-Ramírez, Proc. of SPIE Vol. 8922, 89220X · © 2013
SPIE · CCC code: 0277-786X/13/$18 · doi: 10.1117/12.2035501

Our main objective is to develop a useful tool for the evaluation of the fetal heart, including filtering, segmentation and motion analysis. In this paper, we present preliminary results on the first two tasks: filtering and segmentation. We also evaluate the contribution of the filtering process in the segmentation, i.e., how much the segmentation performance is improved when applying a filtering stage at first. As mentioned, we used two filters based on multiresolution decomposition[15, 23, 24] and a deformable model for the segmentation. We used several cardiac fetal ultrasound images for the assessment. Regarding the cardiac structures, we only present results in the segmentation of the left ventricle.

The rest of the paper is organized as follows. Section 2 presents a general description of the implemented system. Model of the speckle pattern and filtering techniques adopted in this paper are analyzed in section 3. In section 4, the segmentation technique based on active contour models is shown. Results obtained by using the analyzed filters and the segmentation method are described in section 5. Finally, conclusions are presented in section 6.

2. SYSTEM DESCRIPTION

In this research, we carried out the analysis of fetal ultrasound images by using some mathematical models to filter the images in order to reduce the speckle pattern, and to segment the left ventricle structure. As mentioned, the filtering stage is applied to the input images to improve the segmentation task. Figure 1 describes a general scheme of the steps followed in this work. We focus our work in evaluating the segmentation task of fetal ultrasound images in order to extract the left ventricle. The evaluation is made by comparing the segmentation process applied to the original images and their filtered versions.

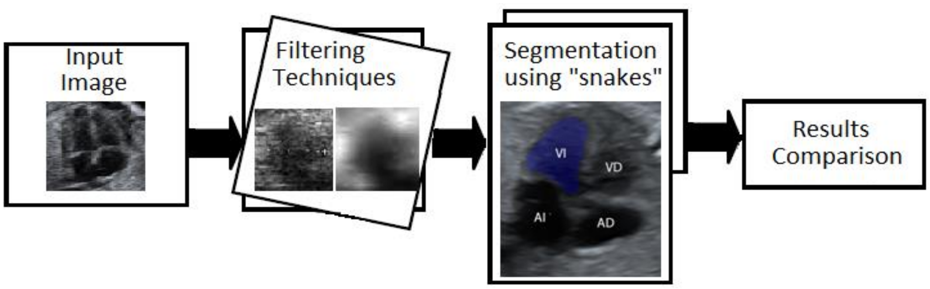

Figure 1. Block diagram of the general system.

As mentioned, the first stage is to filter the images. Here, we have employed two types of filters based on multiresolution analysis. We present the fundamentals of both filters in next section. For the second stage, we used an active contour to segment the left ventricle. Since we intend to make an evaluation of the effect that the filters have in the segmentation task, we address a comparison of the segmentation results obtained with the original and filtered images.

3. FILTERING METHODS FOR ULTRASOUND IMAGES

From an image processing point of view, the speckle pattern is considered as a multiplicative noise that depends on the object tissue and some parameters of the acquisition system[22]. Speckle patterns are presented in the images as granular structures that affect their contrast and visual appearance. With this assumption in mind, several authors[15, 16] have formulated a noise model for speckle patterns as: $g(i, j) = y(i, j) \cdot n(i, j)$, where y corresponds to the noise-free image, n is the speckle noise and g is the corrupted image; (i, j) represents the spatial coordinates. Additive noise is not taken into account because its contribution to the model is low compared with the multiplicative component. A simple way to process the image is to convert the multiplicative model in additive. This can be easily achieved by computing a logarithmic transformation of the image g, which lead to a new model expressed as: $p(i, j) = x(i, j) + N(i, j)$ where $N = \log(n)$, $x = \log(y)$ and $p = \log(g)$. With this representation, methods for suppression of additive noise can be efficiently used.

In our work, we study two types of filters based on multiscale analysis. The first one is based on a Bayesian estimation applied to the coefficients obtained through wavelet decomposition, and the second one is based on the Hermite transform[23, 24]. As a general idea, both methods attend to change the representation space of the images to remove the noise. It is required that the first step is to apply the corresponding transformation. High and low frequency components are obtained with the multiscale representation. Since noise is commonly considered as high frequency details, the filters work directly on these high frequency components. The final process is to return the image to the original space by employing inverse transforms.

3.1 Bayesian filtering method based on the wavelet transform

The Bayesian method analyzed in this work was previously designed by Gupta[15, 21] et al., and it is based on the discrete wavelet transform. Mathematically, we can define this operation for two-dimensional signals (images) as:

$$C(a,b) = C(j,k) = \sum_{x\in Z}\sum_{y\in Z} f(x,y)\, g_{j,k}(x,y) \tag{1}$$

with $a = 2^j$, $b = k2^j$, $j \in N$, $j \in N$. Here, f is the original image, g represents the wavelet function, a is a scaling factor and $C(a,b)$ corresponds to the set of coefficients obtained from the decomposition process, which sometimes are referred as subbands[25, 26]. Several levels of decomposition can be achieved with the wavelet transform. The goal behind the wavelet methods is to perform a better discrimination of the information contained in the image by using other representation. The filters are then applied over the coefficient terms obtained with equation (1). For ultrasound images, the filters work on the high frequency subbands. The reconstruction of the image can be obtained by using an inverse process.

Gupta[15, 21] et al., developed an approach to filter ultrasound medical images. They considered that a Rayleigh distribution[27] characterizes the speckle noise:

$$SN = \frac{n}{\alpha^2}\exp\left(-\frac{n^2}{2\alpha^2}\right) \qquad n \ge 0 \tag{2}$$

On the other hand, the noise-free image is considered to have a Gaussian distribution. In the method, a logarithmic transformation of the image is firstly carried out before applying the wavelet transform. As mentioned, the speckle is thus processed as additive noise. Mihck[28] et al., made an important contribution and demonstrated that the histogram of the wavelet coefficients can be approximated by the zero mean Gaussian distribution:

$$C = \frac{1}{\sigma\sqrt{2\pi}}\exp\left(-\frac{x^2}{2\sigma^2}\right) \qquad -\infty < x < \infty \tag{3}$$

With the last two equations and using the MAP (Maximum a posteriori) theory, Gupta[15, 21] et al., found a final estimation expression to enhance each high frequency subband of the wavelet-based multiscale representation:

$$\hat{x}(y) = sign(y)\cdot\left(\max\left(0, \frac{\left(2|y|\sigma_x^2 + \alpha^2|y| - \sqrt{\alpha^4 y^2 + 4\alpha^2\sigma_x^2 + 4\alpha^2\sigma_x^4}\right)}{2(\alpha^2+\sigma_x^2)}\right)\right) \tag{4}$$

where $\alpha = \sigma/\sqrt{2}$; σ^2 is the variance of the noise which is estimated by $\hat{\sigma}^2 = k\left[\frac{median|y|}{0.6745}\right]$ in the detail coefficients; y corresponds to the first and second level diagonal detail subbands; k is a constant that controls the noise level to be eliminated. Finally, $\hat{\sigma}_x = \sqrt{\max(\hat{\sigma}_y^2 - \hat{\sigma}^2, 0)}$ represents the standard deviation of the signal and $\hat{\sigma}_y^2$ is the variance of the wavelet coefficients. With each subband filtered, the inverse wavelet transform is applied to recover the filtered image.

3.2 Hermite-based filtering method

The Hermite transform is other important mathematical operation that can be used for image multiresolution analysis as well. It can be considered as a special case of polynomial transforms in which the decomposition of an image is obtained by using localized window functions. The polynomial coefficients $L_{m,n-m}(p,q)$ are obtained by the convolution between the original image and the analysis filters defined by: $D_{m,n-m}(x,y) = G_{m,n-m}(-x,-y)\, V^2(-x,-y)$ where $V(x,y)$ is the window function and $G(x,y)$ are the polynomial base functions, which are determined by the window functions that are orthonormal to $V^2(x,y)$. Therefore, the polynomial transform is expressed as:

$$L_{m,n-m}(p,q) = L(x,y) * D_{m,n-m}(x,y) \tag{5}$$

Analogously, there is an inverse process to recover the image. The filtering process through the Hermite-based approach is very similar to the wavelet-based methods. The idea is to apply the corresponding filters in the new representation space. In the algorithm, an energy mask that indicates the edge locations in the image is estimated. The mask is obtained from the first order energy image. This corresponds to the first order coefficients of the Hermite transform. Edge positions of the image are detected with the estimated mask, including those corrupted by speckle. The pixels corresponding to noisy homogeneous areas are then suppressed while image edges are enhanced. The first order energy image corresponding to the convolution of the input image L with the first order derivatives of the Gaussian function can be used to separate edges from noise by using thresholding techniques. The threshold is computed as:

$$T(x,y) = \frac{2\alpha \ln\left(\frac{1}{P_R}\right) L_{00}^2}{AN} \tag{6}$$

where $\alpha = \left| R_L(x,y) * D_{10}(x,y) * D_{01}(x,y) \right|_{x=y=0}$ and R_L is the auto-correlation function of L; P_R is the percentage of noise allowed to remain in the image; L_{00} is the zero order coefficient and A is $(SNR_{1LooK})^2 \approx (1.9131)^2$, $\sigma_l = \mu_l / (\sqrt{N} SNR_{lloop})$; N is the number of looks of L. This algorithm can be reviewed with more details in [23].

4. "SNAKE" - BASED SEGMENTATION

The active contour or "snake" is one of the most employed algorithms for medical image segmentation. Although this technique has several drawbacks that have been extensively demonstrated, we opted to use it in this work since it constitutes a good way to prove the effectiveness and contribution of the filtering approaches in the segmentation task. The active contour is modeled as a parametric curve that aims at minimizing an energy function when the contour is located at the position of the object boundaries. This curve is described as:

$$v(s) = (x(s), y(s)) \tag{7}$$

where $x(s)$ and $y(s)$ are coordinates along the contours and $0 \le s \le 1$. The active contour is then represented as an energy function E_{snake}, which must be minimized to obtain the shape and position of the final contour that segments the image. The energy function is composed by two terms: one codes the image information and the other controls the contour features. This energy function consists of a weighted summation of several terms. They correspond to the forces acting on the contour, which are referred as internal energy E_{int} and external energy E_{ext} functions. The expression of the energy function E_{snake} is denoted by:

$$E_{snake}(v(s)) = \int_{\Omega} \left\{ E_{int}(v(s)) + E_{ext}(v(s)) \right\} ds \tag{8}$$

Finding a solution implies the minimization of the last functional:

$$E_{snake\_min} = min \int_{\Omega} \{ E_{int}(v(s)) + E_{ext}(v(s)) \} \, ds \tag{9}$$

The behavior or the regularity of the curve is controlled with the internal energy, which is defined as $\alpha E_{cont}(v(s)) + \beta E_{curv}(v(s)) = \alpha(v_s(s)) + \beta(v_{ss}(s))$, where $E_{cont}(v(s))$ measures the elasticity of the "snake", $E_{curv}(v(s))$ determines the energy of the curvature, v_s and v_{ss} represent the first and second derivative operations. On the other hand, the external energy is considered as the image energy E_{ima}, which is used to attract the curve to the boundary features in the image[29-32].

$$E_{snake\_min} = min \int_{\Omega} \{ \alpha E_{cont}(v(s)) + \beta E_{curv}(v(s)) + \gamma E_{ima}(v(s)) \} \, ds \tag{10}$$

where α, β and γ are weight parameters that control the contribution of each term. Elasticity and rigidity are controlled by the internal energy. For the minimization of the functional, variational calculus[33-34] is often used.

5. MATERIALS

For the evaluation of the methods we have used 7 ultrasound images of the fetal heart. The images were acquired with a Voluson E8 ultrasound system of General Electric with a resolution of 0.18 mm per pixel. The image size is 224 x 260. To assess the filtering algorithms, we also created a phantom image with the segmented structures made by the expert in one of our dataset of real ultrasound images. Speckle noise was manually added to the phantom in order to address a quantitative analysis.

6. RESULTS

We have evaluated the two explained filtering techniques by using the phantom image degraded with the simulated speckle noise. In figures 2a and 2b, we illustrate this sample image and its noisy version. For the quantitative analysis, we also compare the multiresolution-based methods with other common approaches as the anisotropic and wiener filters. Several metrics are obtained for each result of the analyzed filters. Signal to noise ratio (SNR), peak signal-to-noise ratio (PSNR) and correlation coefficient (CoC) are calculated to compare the performance. Table 1 depicts the quantitative analysis.

Table 1. Quantitative results of the filtering techniques.

	Evaluated Parameters		
Method	**SNR(dB)**	**PSNR**	**CoC**
Input Image with speckle noise	2.5384	12.7040	0.8545
Wiener	2.9807	12.8385	0.9238
Anisotropic diffusion	3.2135	12.8899	0.9606
Bayesian	2.9933	12.9461	0.9615
Hermite	**5.3023**	**19.2529**	**0.9779**

Visual results for the two multiscale-based filters are also illustrated for the synthetic and real images (see figures 2 and 3). It is noticed that a better performance is obtained with the Hermite-based approach. This filter is more efficient in removing speckle patterns while the edges of the images are preserved (figure 3f). Subsequently, the original image and the filtered images are evaluated and compared. Figures 3b, 3c and 3e show the image energy obtained by using a common and simple gradient function. In our algorithm, this gradient operator is used as the external energy in the "snake" functional.

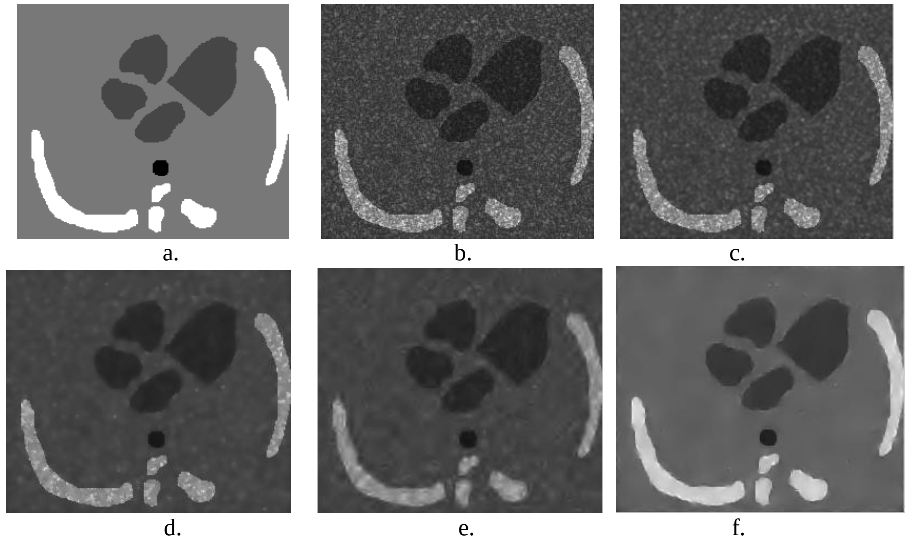

Figure 2. Results obtained for the phantom image, a. Noise-free Image, b. Speckle Simulated, c. Wiener, d. Anisotropic diffusion, e. Wavelet-based Bayesian method, f. Hermite-based method.

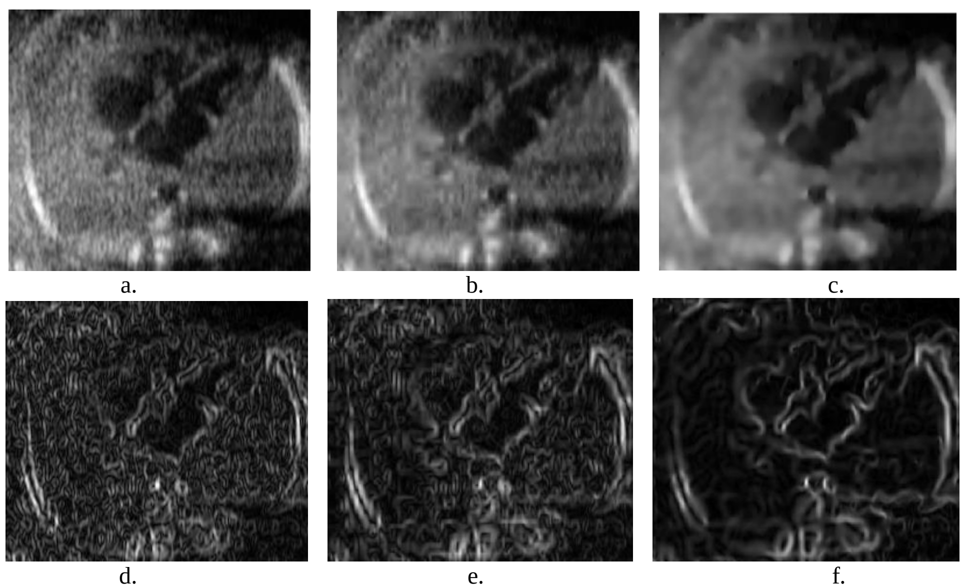

Figure 3. Original and filtered images and their respective image energy: a) Original Image, b) Filtered with the wavelet-based Bayesian approach, c) Filtered with the Hermite-based method, d) Image energy E_{ima} of the original, e) Image Energy E_{ima} of the filtered image using the wavelet-based Bayesian method Filtered with the Hermite-based method and f) Image Energy E_{ima} of the filtered image using the Hermite-based method.

From the image energy illustrated in figure 3, we can see that the segmentation process becomes a difficult task in the original image. The high variations caused by the speckle noise prevent the gradient function from extracting the boundaries of the left ventricle.

The "snake" model has been implemented and evaluated on fetal ultrasound images in different time sequences using the original data and the filtered versions. Figure 4 shows an example of the initial contour used in the algorithm which was put on one of the images of our dataset. The initialization is manual and is made by selecting a control point in the image to draw a closed circle with a specific radius.

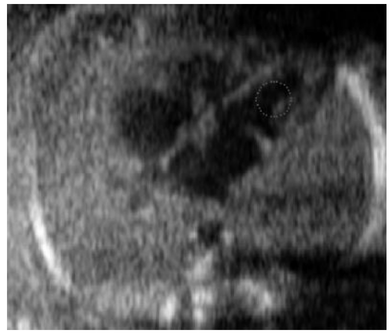

Figure 4. Initial contour inside the left ventricle

Visual results of the performance obtained with the segmentation method for two images are described in figure 5. Several results are illustrated by using the original image and the filtered versions with the multiresolution-based approaches. In the case of the filtered images, we found acceptable results of the segmented structure. The results are illustrated in figures 5b, 5c, 5e and 5f. The convergence of the "snake" was faster in the filtered images as well.

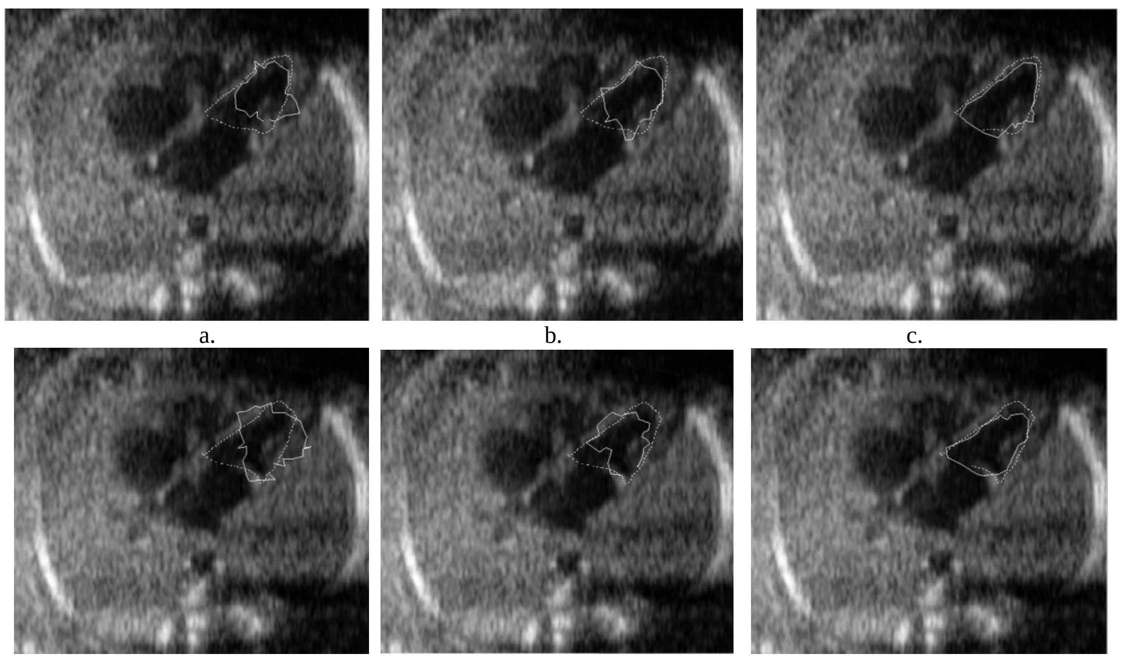

a. b. c.

d. e. f.

Figure 5. Segmentation results in two echocardiographic images of the fetal heart. The solid line is the automatic segmentation and the dotted lines describes the manual segmentation made by the expert: a) Original Image 1, b) Filtered image 1 with the wavelet-based Bayesian approach, c) Filtered image 1 with the Hermite-based method, d) Original Image 2, e) Filtered image 2 with the wavelet-based Bayesian approach and f) Filtered image 2 with the Hermite-based method.

Quantitative analysis is also used to evaluate the segmentation results. Euclidean distance metric is employed for this task in which a comparison with the expert segmentation is made. Table 2 describes the obtained results in the process of extracting the left ventricle in all the images of our dataset by using the original images and the filtered one with the wavelet-based method and the Hermite-based approach. In this work, we only include some preliminary results about the methods depicted in the last section. As can be seen from the analysis made, the segmentation is improved using filtered images. The best result was subsequently obtained with the filtered images employing the Hermite based method.

Table 2. Quantitative analysis of the segmentation results.

	Original Image (pixels) mean ± std	Wavelet transform (pixels) mean ± std	Hermite Transform (pixels) mean ± std
Image 1	5.40 ± 4.58	4.21 ± 2.63	3.60 ± 2.23
Image 2	4.76 ± 4.05	3.74 ± 3.10	3.24 ± 2.57
Image 3	4.13 ± 3.80	4.09 ± 3.28	2.79 ± 2.33
Image 4	6.37 ± 4.26	4.39 ± 3.44	3.36 ± 3.29
Image 5	6.36 ± 5.98	5.97 ± 4.86	4.70 ± 4.98
Image 6	6.22 ± 6.33	6.20 ± 5.99	5.54 ± 5.77
Image 7	7.50 ± 8.14	5.98 ± 6.64	4.81 ± 5.82

7. CONCLUSIONS

We have implemented a system for the filtering and segmentation process of echocardiographic fetal images. The system includes two multiresolution-based filtering methods and an active contour model for segmentation. Filtering techniques visually enhance the appearance of ultrasound images and help in the segmentation process. The best performance was achieved with the approach based on the Hermite transform which is a robust multiresolution despeckling method that preserves important features in the ultrasound images. The wavelet-based method has proved to be efficient in reducing the speckle pattern, but the image edges are considerably blurred. Therefore, preliminary results in this research conclude that the filtering techniques used here improve substantially the segmentation results. In future works, we propose to address a better analysis about the image features taking advantage of the statistical properties. We also plan to consider more robust algorithms for the segmentation of ultrasound images of the fetal heart.

ACKNOWLEGEMENT

This work was supported by UNAM grant PAPIIT IN113611 and UNAM-CEP. Vargas-Quintero L. also thanks Colciencias. Authors thank to National Institute of Perinatology in México for providing the ultrasound fetal images.

REFERENCES

[1] S. Laurent, P. Boutouyrie, R. Asmar, I. Gautier, B. Laloux, L. Guize, P. Ducimetiere, and A. Benetos, "Aortic stiffness is an independent predictor of all-cause and cardiovascular mortality in hypertensive patients, " *Hypertension*, 37, 1236–1241 (2001).

[2] J. Ophir, S. Alam, B. Garra, F. Kallel, E. Konofagou, T. Krouskop, C. Merritt, R. Righetti, R. Souchon, S. Srinivasan, and T. Varghese, "Elastography: Imaging the Elastic Properties of Soft Tissues with Ultrasound, " Medical Ultrasound, 29, 155–171 (2002).

[3] A. A. Bini, M. S. Bhat, "Despeckling low SNR, low contrast ultrasound images via anisotropic level set diffusion," Multidimensional Systems and Signal Processing, 1-25 (2012).

[4] A. F. Frangi, D. Rueckert, and J. S. Duncan. "Threedimensional cardiovascular image analysis," IEEE Transactions on Medical Imaging, 21(9), 1005–1010 (2002).

[5] Yefeng Zheng, Adrian Barbu, Bogdan Georgescu, Michael Scheuering, and Dorin Comaniciu, "Four-Chamber Heart Modeling and Automatic Segmentation for 3D Cardiac CT Volumes Using Marginal Space Learning and Steerable Features, " IEEE Transactions on Medical Imaging, 27(11) , 1668–1681 (2007).

[6] Hammoude, A., "Endocardial border identification in two dimensional echocardiographic image:Review of methods, " Computer Medical Imaging Graphic, 22(3), 181-193 (1998).

[7] Dydenko I., Friboulet, D, Gorce, J., D'hooge, J., Bijnens, B., and Magnin I.E., "Towards ultrasound cardiac image segmentation based on the radiofrequency signal," Medical Image Analysis, 7(3), 353-367 (2003).

[8] Noble J. and Boukerroui Djamal, "Ultrasound Image Segmentation: A Survey," IEEE Transactions on Medical Imaging, 25(8), 987-1010 (2006).

[9] Kass, M., Witkin, A., Terzopoulos, D., "Snakes: active contour models," International Journal Computer

Vision, 1, 321-331 (1987).
[10] Cohen, L., Cohen, I., "Finite-element methods for active contour model and balloons for 2D and 3D images," IEEE Transactions on Pattern Analysis and Machine Intelligence, 15(11), 617-634 (1993).
[11] Gunn, S., Nixon, M., "A robust snake implementation via a dual active contour," IEEE Transactions on Pattern Analysis and Machine Intelligence, 19(1), 63-68 (1997).
[12] Lilian Ji, Hong Yan, "Attractable snakes based on the greedy algorithm for contour extraction," Pattern Recognition, 35, 791-806 (2002).
[13] Smith, S. W., Wagner, R. F., Sandrik, J. M. and Lopez, H., "Low contrast detectability and contrast/detail analysis in medical ultrasound," IEEE Transactions on Sonics and Ultrasonics 30(3), 164–173 (1983).
[14] Yu, Y. and Acton, S.T., "Speckle reducing anisotropic diffusion," IEEE Trans. Image Process. 11 (11), 1260–1270 (2002)
[15] Gupta, S., Chauhan, R.C. and Saxena, S.C., "Homomorphic wavelet thresholding technique for denoising medical ultrasound images," Taylor & Francis Int. J. Med. Eng. Technol. 29 (5), 208–214 (2005).
[16] Pižurica, A., Philips, W., Lemahieu and I., Acheroy, M., "A versatile wavelet domain noise filtration technique for medical imaging," IEEE Trans. Medical Imaging 22 (3), 323-331 (2003).
[17] Yue, Y., Croitoru, M.M., Bidani, A., Zwischenberger, J.B. and Clark, J.W., "Non-linear multiscale wavelet diffusion for speckle suppression and edge enhancement in ultrasound images," IEEE Trans. Medical Imaging 25 (3), 297-311 (2006).
[18] Achim, A., Bezerianos, A., and Tsakalides, P.," Novel Bayesian multiscale method for speckle removal in medical ultrasound images," IEEE Transactions on Medical Imaging 20(8), 772-783 (2001).
[19] Donoho, D. L., "De-noising by soft-thresholding," IEEE Trans. Inform. Theory 41(3), 613–627 (1995).
[20] Grace Chang, S., "Adaptive Wavelet Thresholding for Image Denoising and Compression," IEEE Trans. Image Processing, 9(9), 1532-1546 (2000).
[21] Gupta, S., "Locally adaptive wavelet domain Bayesian processor for denoising medical ultrasound images using Speckle modeling based on Rayleigh distribution," IEE Proc.-Vis. Image Signal Process 152(1), 129-135 (2005).
[22] Kalaivani Narayanan, S. and Wahidabanu, R.S.D., "A View on Despeckling in Ultrasound Imaging," International Journal of Signal Processing Image Processing and Pattern Recognition 2 (3), 85-98 (2009).
[23] Escalante-Ramírez, Boris and López-Caloca, Alejandra A. "The Hermite Transform: An Efficient Tool for Noise Reduction and Image Fusion in Remote Sensing in Signal and Image Processing for Remote Sensing," Taylor and Francis, 537-555 (2006).
[24] Silván-Cárdenas, José L., Escalante-Ramírez, Boris, "The multiscale hermite transform for local orientation analysis," IEEE Transactions on Image Processing 15(5), 1236-1253 (2006).
[25] B.J., Leiner, V.Q., Lorena, T.M., Cesar, M.V., Lorenzo, "Microcalcifications Detection System through Discrete Wavelet Analysis and Image Enhancement Techniques," Proc. 40th Southeastern Symposium on System Theory 40, 118-121 (2008).
[26] Barba, L., Vargas, L., Torres, C., Mattos, L., "Digital Correlation based on Wavelet Transform for Image Detection," J. Phys.: Conf. Ser. 274(1), 1-13 (2011).
[27] Papoulis, A., [Probability random variables and stochastic processes] MHL, New York, (1991).
[28] Mihçak, M.K. Kozintsev, I., Ramchandran, K. and Moulin, P., "Low complexity image denoising based on statistical modeling of wavelet coefficients," IEEE Signal Process. Lett. 6(12), 300-303 (1999).
[29] C. Y. Xu, J.L. Prince, "Snakes, shapes and gradient vector flow," IEEE Transaction Image Process. 7(3), 359-369 (1998).
[30] V. Caselles, R. Kimmel, G. Sapiro, "Geodesic active contours," International Journal Computer Vision 22 (1), 61-79 (1997).
[31] T McInerney, D. TEerzopoulos, "Topologically adaptable snakes," Proceedings of IEEE ICCV-95, 840-845 (1995).
[32] R. Ronfard, "Region based strategies for active contour models," International Journal Computer Vision 13(2), 229-251(1994).
[33] G. Aubert and P. Kornpbrost, [Mathematical problems in image processing: Partial differential equations and the calculus of variations] Springer, (2006).
[34] A. Mitiche and I. Ben Ayed, [Variational and Level Set Methods in Image Segmentation], Springer Topics in Signal Processing, (2010).
[35] Vargas-Quintero, Lorena, Escalante-Ramírez, Boris and Arámbula Fernando, "Filtering and Detection of Low Contrast Structures on Ultrasound Images," Processing SPIE 8436, 1-11 (2012).